

Title	Experimental characterization of low temperature solid oxide cell stack
Author(s)	Tallgren, Johan; Himanen, Olli; Nojonen, Matti
Citation	ECS Transactions. Electrochemical Society. Vol. 78 (2017) No: 1, Pages: 3103-3111
Date	2017
URL	http://dx.doi.org/10.1149/07801.3103ecst
Rights	This post-print version of the article may be downloaded for personal use only.

VTT
<http://www.vtt.fi>
P.O. box 1000
FI-02044 VTT
Finland

By using VTT Digital Open Access Repository you are bound by the following Terms & Conditions.

I have read and I understand the following statement:

This document is protected by copyright and other intellectual property rights, and duplication or sale of all or part of any of this document is not permitted, except duplication for research use or educational purposes in electronic or print form. You must obtain permission for any other use. Electronic or print copies may not be offered for sale.

Experimental Characterization of Low Temperature Solid Oxide Cell Stack

J. Tallgren^a, O. Himanen^a, M. Noponen^b

^a VTT Technical Research Centre of Finland Ltd, P.O. Box 1000, FI-02044, Finland

^b Elcogen Oy, Niittyvillankuja 4, 01510 Vantaa, Finland

Reversible solid oxide cell (rSOC) and solid oxide electrolysis (SOE) are gaining growing interest because they can convert both electricity into a chemical fuel and fuel back to electricity with high efficiency. This work summarizes the electrochemical performance characterization of Elcogen E350 stack both in fuel cell and electrolysis modes. Elcogen E350 stack is composed of 15 unit layers all having a 121 cm² active electrode area. The electrochemical characterization is conducted in temperature region 650–700 °C and with varying current densities, multiple hydrogen-to-steam ratios, reactant utilizations and air flow rates. Results indicate that the stack can be used not only as a fuel cell but also in electrolysis mode. It is capable to be operated up to 1.0 A cm⁻² current below 700 °C and can be operated also with high reactant utilization in electrolysis mode.

Introduction

Solid oxide cells (SOC) have been extensively developed as a low-carbon, efficient energy production method as solid oxide fuel cells (SOFC) but emerge now also in the use as solid oxide electrolysis cells (SOEC). The increasing share of solar and wind energy leads to a mismatch between energy supply and demand, which calls for efficient energy storage technologies. SOEC systems possess several advantages as means for energy storage, such as a high efficiency due to the high operating temperature, high purity hydrogen production and capability for co-electrolysis. The high operating temperature of 600–850 °C is beneficial as a significant part of the required energy can be supplied as heat, yielding efficiencies above 90%. The high temperature favours also reaction kinetics and ohmic conductivity. Waste heat or surplus power from power plants during off-peak hours could be utilized. (1–3) Apart from producing hydrogen via water electrolysis, the SOEC can produce syngas via co-electrolysis, where a mixture of steam and carbon dioxide is fed to the system. Syngas is used as a raw material in synthesis of methane, fuels and chemicals. Combined with renewable energy, water electrolysis is probably the cleanest hydrogen production method today (4). In addition, reversible solid oxide cells (rSOC) are gaining growing interest as they can be used for both energy storage and production, although this was shown already in the 1980s (5). There are also reports that the reversible operation may enhance the performance stability and suppress electrode degradation taking place in SOEC mode (6).

The electrochemical reactions in a SOEC are opposite to the SOFC. To avoid confusions between the terms of anode and cathode in fuel cell and electrolyser use, the electrodes are here called hydrogen electrode and air electrode. In a SOEC, steam is fed to the

hydrogen electrode and air to the air electrode. Often a part of hydrogen is added to the steam to ensure reducing conditions for the nickel electrode. Hydrogen is produced at the fuel electrode and oxygen at the air electrode. Oxygen ions pass through the electrolyte to the air electrode. In case of co-electrolysis, a mixture of carbon dioxide and steam is fed to the hydrogen electrode where carbon monoxide and hydrogen is produced. For water electrolysis, the half-cell reaction at the fuel electrode follows (Eq. 1)



and at the air electrode (Eq. 2)



The thermoneutral potential level is calculated as

$$U_{TN} = \frac{-\Delta H}{n F} \quad [3]$$

where ΔH is the change in enthalpy and F is Faraday's constant. Above U_{TN} the overall electrolyser reaction is exothermic and below U_{TN} the overall reaction is endothermic.

The material requirements are similar for SOECs as for SOFCs and the materials are therefore developed based on those for SOFCs. Long-term degradation is still an issue and the lowest reported degradation is according to Moçoteguy et al twice as high as for SOFCs (~1.7% / kh) (2). Recent literature on SOEC stack characterization include, among others, Diethelm et al (7) who have reported characterization of two 6-cell SOLIDPower stacks in 600–700 °C, Alenazey et al (8) who have reported the performance of a 6-cell stack at 750 °C and Kotisaari et al (9) who have reported the characterization of a 6-cell stack at 750–800 °C.

This work summarizes for the first time the electrochemical performance characterization of Elcogen E350 stack both in fuel cell and electrolysis operation. The electrochemical characterization is conducted in temperature region 650–700 °C and with varying current densities, multiple hydrogen-to-steam ratios, reactant utilizations and air flow rates.

Experimental

The characterized stack was an Elcogen E350 stack, composed of 15 hydrogen electrode supported NiO/YSZ–YSZ–GDC–LSC cells with an active area of 121 cm² (10). Stack characterization was performed in a highly instrumented and automated in-house built stack test station, capable of both SOFC and SOEC testing. The stack was placed in a furnace (custom made, MeyerVastus) and connected via a set of relays to either an electronic load (ElektroAutomatik EA-EL 9160-200) or a power supply (DeltaElektronika SM30-150 D). The relays ensured that the power supply and load could not be connected simultaneously and made fast switching between fuel cell and electrolysis mode possible. Gases were fed through mass flow controllers (Bronkhorst EL-FLOW series) and steam

was supplied with an evaporator (custom-made, EBZ) and a liquid water flow controller (Bronkhorst Liqui-Flow). Humidity (Vaisala HMT337) and oxygen content (SICK TRANSIC100LP) was measured at air inlet and outlet. Exhaust gas flow and humidity from the hydrogen electrode was measured with Vaisala HMT337 humidity sensor and Höntzsch FA volumetric gas flow meter, corrected for temperature and pressure. Cell voltages of each individual cell were measured.

The electrochemical characterization of the Elcogen E350 stack was performed by measuring a multiple of polarization curves at different temperatures and with varying current densities, multiple steam-to-hydrogen ratios, reactant utilizations and air flow rates. Table I presents the intervals of the varied parameters. Hydrogen was added to the steam to ensure a reducing atmosphere for the nickel hydrogen electrode. Air flow was varied so that the lambda value, calculated as air flow divided by steam flow, was varied between 3.0 and 4.3. Apart from the test set with varying reactant utilization (RU), the maximum RU was kept at 60%. Polarization curves were measured with a current ramp rate of 1.0 A min^{-1} .

TABLE I. Presentation of the varied operation conditions in electrolysis mode.

Varied parameter	Min value	Step	Max value
Temperature / °C	650	25	700
Current density / A cm^{-2}	0.5	0.25	1.0
Hydrogen-to-steam ratio	10%	10%	30%
Reactant utilization	40%	5%	80%

Prior to measuring the different SOEC polarization curves, operation in rSOC mode was demonstrated in the beginning of the test at $650 \text{ }^\circ\text{C}$. Here a polarization curve in fuel cell mode was recorded and as the current was returned to zero, the relays were switched and a polarization curve in electrolyser mode could be recorded. In rSOC mode the stack was fuelled with 50%/50% $\text{H}_2/\text{H}_2\text{O}$, so that the maximum fuel utilization was 47% and maximum reactant utilization was 80%.

Results and discussion

After transport from manufacturer and prior to heating, the stack was pressurized to detect leakages. The stack was determined satisfactorily leak-tight and was heated with a ramp of 60 K min^{-1} . At first, a fuel cell polarization curve was recorded and compared to the quality assurance test performed by manufacturer. As these showed same results, the characterization test was started.

Figure 1 presents the rSOC polarization curve recorded without modifying fuel feed ($7.76 \text{ l}_\text{N} \text{ min}^{-1} \text{ H}_2\text{O}$ and $7.76 \text{ l}_\text{N} \text{ min}^{-1} \text{ H}_2$) between SOFC and SOEC operation at $650 \text{ }^\circ\text{C}$. Air feed was $33 \text{ l}_\text{N} \text{ min}^{-1}$ corresponding to a lambda value of 4.3. In fuel cell operation, the maximum current drawn from the stack was 35 A (0.29 A cm^{-2}) and in electrolysis mode 59 A (0.49 A cm^{-2}), corresponding to fuel utilization of 47% and reactant utilization of 80%. The average cell voltage at maximum current density in fuel cell mode was 830 mV and in electrolysis mode 1385 mV . Theoretical Nernst potential calculated with the stack inlet parameters is 988 mV and the measured open circuit voltage was 985 mV .

This indicates either a leakage in the stack or inaccuracy of input gas flow rates. Thermoneutral voltage (U_{tn}) at the given input conditions in the electrolysis mode is 1282 mV. Corresponding current density is 0.30 A cm^{-2} . The polarization curve shows that the stack is capable of operate both as SOFC and SOEC and operation can quickly be switch between the modes.

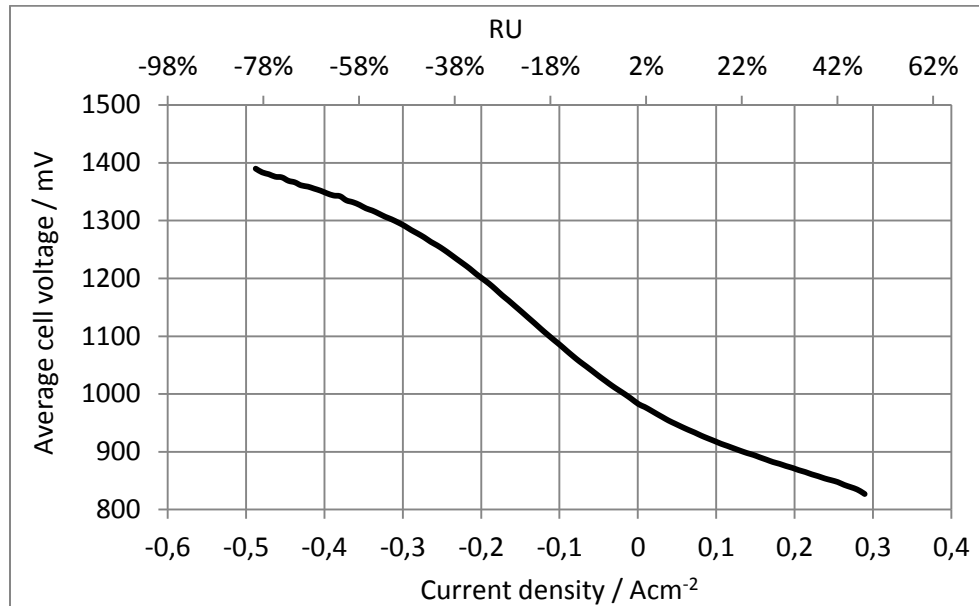


Figure 1. rSOC polarization curve at $650 \text{ }^\circ\text{C}$. Fuel inlet: $7.76 \text{ l}_N \text{ min}^{-1}$ of H_2 and $7.76 \text{ l}_N \text{ min}^{-1}$ of H_2O . Air inlet: $33 \text{ l}_N \text{ min}^{-1}$.

SOEC polarization curves recorded with different operating temperatures and inlet air feeds are compared in Figure 2. The graph clearly depicts that higher operating temperature is beneficial for the stack performance. OCV is reduced at higher temperatures (905, 895, 883 mV) and the area specific resistance is simultaneously decreased ($1.37, 1.18, \text{ to } 1.04 \text{ } \Omega \text{ cm}^2$), defined as a slope from $0.1 \text{ to } 0.2 \text{ A cm}^{-2}$. The ASR defined above thermoneutral potential level shows significantly lower values than below the thermoneutral voltage, i.e. $0.14 \text{ } \Omega \text{ cm}^2$ (650°C), $0.10 \text{ } \Omega \text{ cm}^2$ (675°C), and $0.11 \text{ } \Omega \text{ cm}^2$ (700°C). The difference in the current-voltage curve slope is because below U_{tn} overall electrolyser reaction is endothermic and thus the stack temperature is decreased compared to the furnace and gas inlet temperatures. Above U_{tn} the overall stack reactions are exothermic and the stack starts to produce excess heat and thus stack outlet is heated compared to the stack inlet side. The same thermal phenomenon can be seen when the stack is operated at different air flow rates. The stack inlet conditions are otherwise same, i.e. temperatures and concentrations, and only the air flow rate is changed. Below U_{tn} , higher air flow rate result in better performance as the increased enthalpy input through air prevents the stack from cooling down as much as with lower air flow rate. On the other hand above U_{tn} , higher air flow rate prevents the stack from heating as much as with lower air flow rate and thus the stack performance is enhanced by lower air flow rate. The effect is most prone at 650°C indicating that the temperature correlation to stack performance is not linear in nature between $650 - 700 \text{ }^\circ\text{C}$. The effect is also demonstrated in Figure 3, which shows outlet fuel and air temperatures as well as current density during a polarization curve measurement. At first, the outlet gas temperatures are decreasing but at around 0.3 A cm^{-2} the temperatures start to increase.

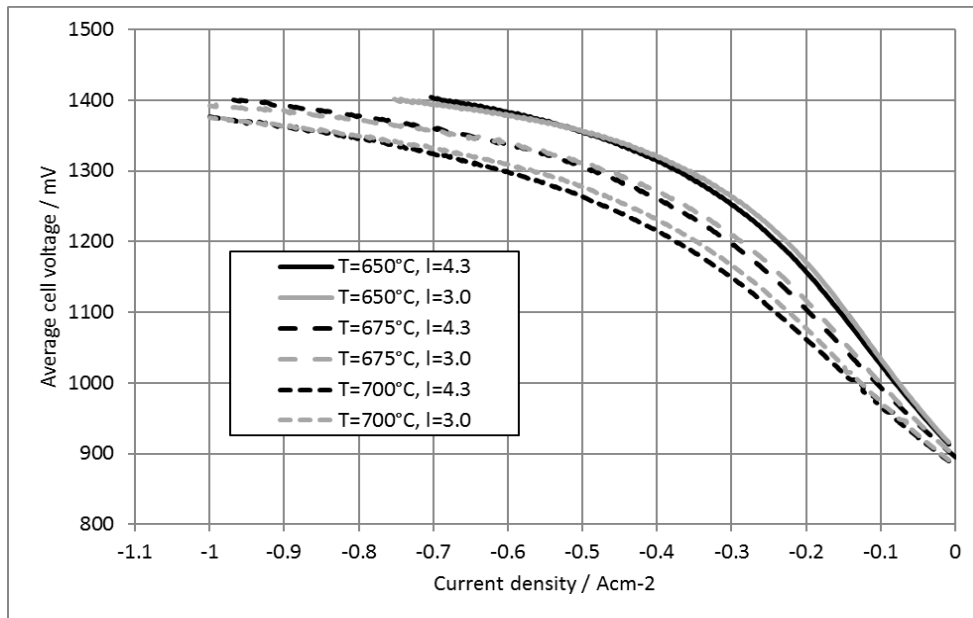


Figure 2. Different operating temperatures and air flow rates. Fuel inlet: $21.08 \text{ l}_N \text{ min}^{-1} \text{ H}_2\text{O}$ and $2.34 \text{ l}_N \text{ min}^{-1} \text{ H}_2$ (10% hydrogen-to-steam ratio).

Figure 2 shows clearly that the stack is capable to be operated up to 1.0 A cm^{-2} already at $675 \text{ }^\circ\text{C}$ and 0.75 A cm^{-2} at $650 \text{ }^\circ\text{C}$. The average cell voltage at $700 \text{ }^\circ\text{C}$ and 1.0 A cm^{-2} was 1394 mV . Alenzey et al reported approximately 1260 mV at 1.0 A cm^{-2} with higher operation temperature of $750 \text{ }^\circ\text{C}$. Fuel composition and feed was similar but air feed twice smaller. Kotisaari et al reported average cell voltage of 1330 mV at 0.5 A cm^{-2} and $700 \text{ }^\circ\text{C}$ with similar fuel feed and 50% higher air feed. For corresponding operation conditions, the average cell voltage measured in this work was 1275 mV . At this operation point the specific energy consumption was $3.05 \text{ kWh/m}^3_{\text{H}_2}$.

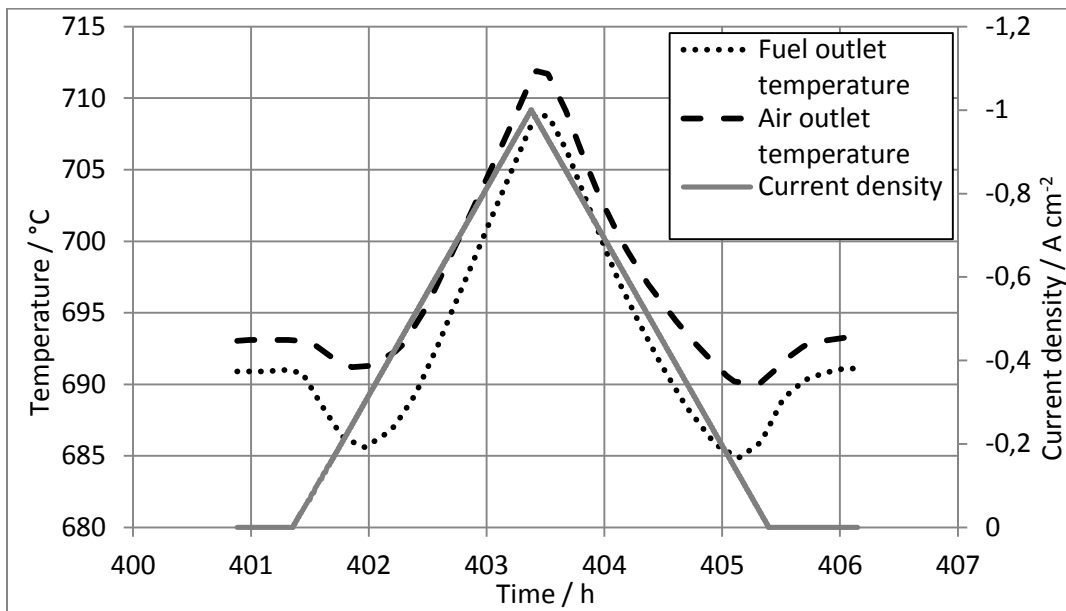


Figure 3. Air and fuel outlet temperatures during a polarization curve measurement at $700 \text{ }^\circ\text{C}$. Fuel inlet: $21.08 \text{ l}_N \text{ min}^{-1} \text{ H}_2\text{O}$ and $2.34 \text{ l}_N \text{ min}^{-1} \text{ H}_2$ (10% hydrogen-to-steam ratio). Air inlet feed: $63 \text{ l}_N \text{ min}^{-1}$ (λ 3.0).

Polarization curves at different hydrogen molar fraction (10%, 20% and 30%) are presented in Figure 4. Furnace temperature was 700 °C and steam flow rate 21.3 l_N min⁻¹. Nernst potentials at the given stack inlet conditions are 880, 914, and 937 mV as the measured OCV values were 883, 918, 941 mV, respectively. At 1.0 A cm⁻², measured voltages were 1375, 1382, 1392 mV. The voltage difference stemming from the different steam partial pressures is maintained over the whole polarization curve but the magnitude diminishes as current is increased. The voltage difference between OCV 10–20% was 35 mV and 10–30% it was 58 mV as the voltage differences at 1.0 A cm⁻² were 7 and 17 mV, respectively. The resulting increased power consumption at 1.0 A cm⁻² is 0.85 W/[unit layer] and 2.1 W/[unit layer], respectively. Hydrogen molar fraction should be minimized in the stack inlet in order to maximize system efficiency. On the other hand, it is known fact that at low hydrogen molar fractions (high steam partial pressures), nickel agglomeration starts to increase unit cell degradation. In addition, it might be beneficial to recycle electrolyser product gas back to stack inlet from the heat balance, reactant utilization and hydrogen concentration point of views. Current densities at thermoneutral potential were 0.513, 0.488 and 0.455 A cm⁻².

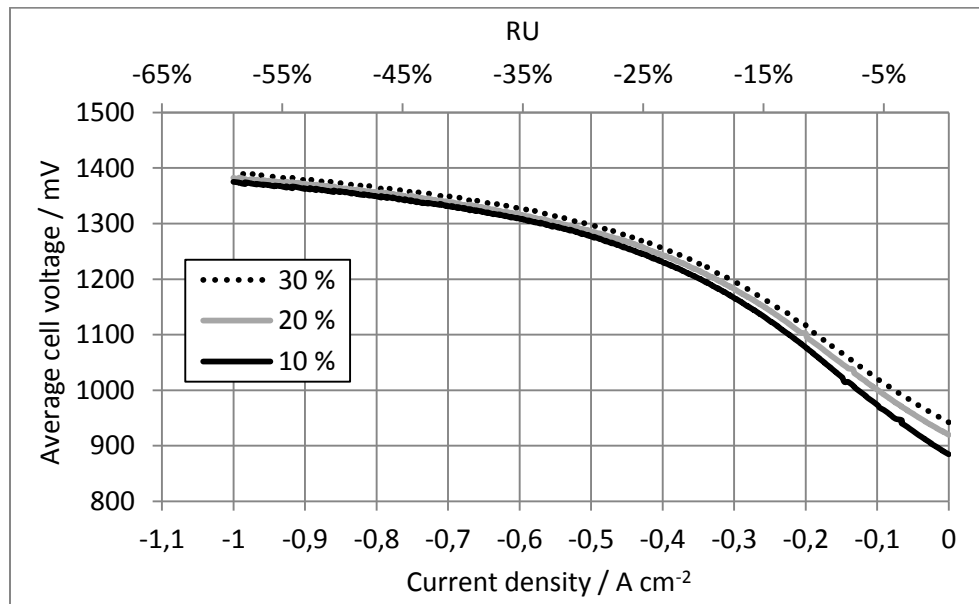


Figure 4: Different hydrogen-to-steam ratios at 700 °C. Air inlet: 63 l_N min⁻¹ corresponds to lambda 3.0.

Figure 5 presents a set of polarization curves recorded when varying the maximum reactant utilization. The polarization curves are recorded up to 1.0 A cm⁻². As seen in the graph, cell voltages increase with increasing reactant utilization. The difference between the curves corresponding to 40% RU and 80% is 40 mV. However, the graph demonstrate that SOEC operation with high RU of 80% is possible and the optimal operation point is a balance between energy demand for steam supply and electricity demand for the electrolysis reaction, as well as long-time stack performance stability.

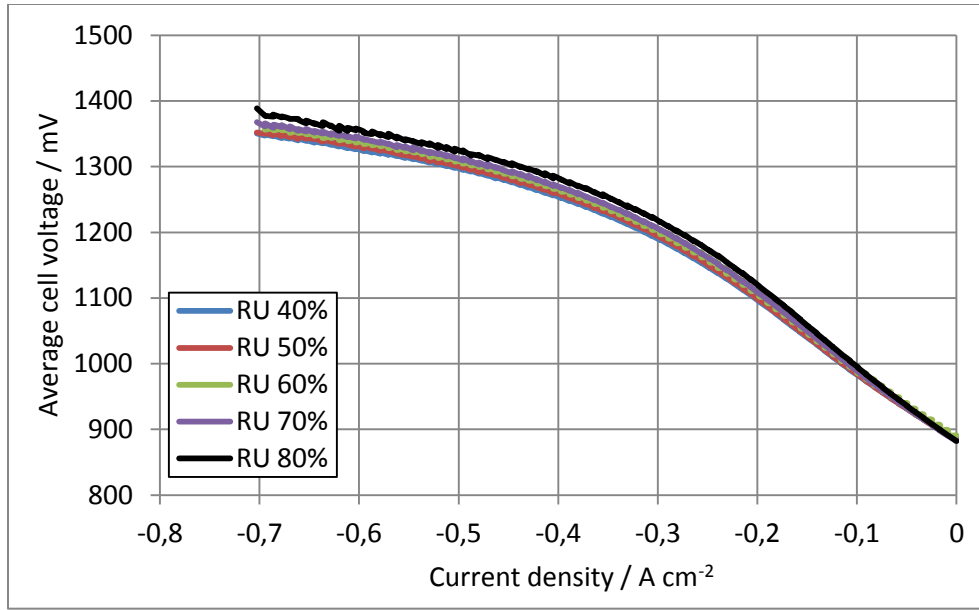


Figure 5. Polarization curves with different maximum reactant utilizations at 700 °C. Air flow was held constant at 63 l_N min⁻¹, i.e. lambda varied from 2.8 to 5.7.

Figure 6 depicts partial pressure of steam against measurement time with two methods. Measurement record is from the polarization measurement conducted at 700 °C furnace temperature, 1.0 A cm⁻² maximum current density, 3.0 lambda, and 0.1 H₂ molar fraction. The measured value is read with the Vaisala HMT337 and calculated value is determined as

$$p_{H_2O} = p_{ambient} \frac{\dot{n}_{H_2O}^{(inlet)} - In_{cell}/2F}{\dot{n}_{H_2O}^{(inlet)} + \dot{n}_{H_2}^{(inlet)}} \quad [4]$$

where $p_{ambient}$ is measured ambient pressure [hPa], $\dot{n}_{H_2O}^{(inlet)}$ is steam flow rate in [mol/s], $\dot{n}_{H_2}^{(inlet)}$ is hydrogen flow rate in [mol/s], I is current [A], n_{cell} is number of cells in stack (15 cells) and F is Faraday's constant (96485 As mol⁻¹). The deviation between the measured and calculated values is between 4 to 22 hPa and the measured value is always smaller than the calculated one. Thus, it means gas leakage in the stack between the air and fuel compartments is negligible compared to the measurement accuracy of the humidity sensor, current measurement and the flow meters. If leakages would be pronounced, hydrogen would react with oxygen producing more steam and thus partial pressure of steam should be higher. Therefore in Elcogen E350 stack and given conditions, hydrogen production can be estimated with reasonable accuracy directly from current measurement by using Faraday's law.

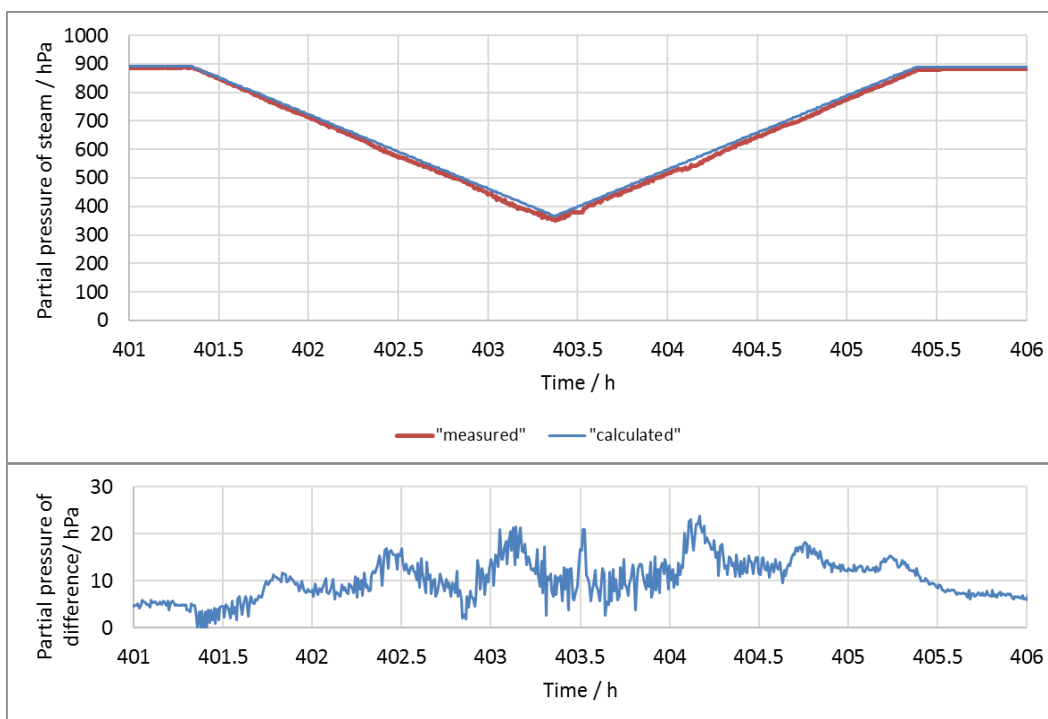


Figure 6. Partial pressure of steam measured and calculated (top) and the deviation between these (bottom) from stack outlet during a polarization curve measurement.

Summary

An Elcogen E350 stack was characterized in both rSOC and SOEC operation. The electrochemical characterization was performed by recording polarization curves in the temperature region 650–700 °C. The effects of hydrogen-to-steam ratios in fuel, air inlet feed and reactant utilization were studied. In SOEC mode, the stack could be operated up to 1.0 A cm⁻² already at 675 °C and 0.75 A cm⁻² at 650 °C. Reactant utilization of 80% was demonstrated. Compared with characterization results in literature, the stack performance was good and the performance values were comparable to reported results. Additionally, the operation temperature of the stack is comparatively low which is beneficial for delaying degradation. The thin 3 μm electrolyte supports good performance at lower temperatures. Thus, the characterization showed that the stack is fully functional in both rSOC and SOEC operation. Further work includes long-term degradation testing and performance characterization in co-electrolysis.

References

1. A. Hauch et al, *J. Mater. Chem.*, **18** (2008).
2. P. Moçoteguy and A. Brisse, *Int. J. Hydrogen Energy.*, **38** (2013).
3. M. Ni et al, *Int. J. Hydrogen Energy.*, **33** (2008).
4. M.A. Laguna-Bercero, *J. Power Sources.*, **203** (2012).
5. M. Mogensen et al, *Ceram. Eng. Sci. Proc.*, (2008).
6. K. Chen and S.P. Jiang, *J. Electrochem. Soc.*, **163** (2016).
7. S. Diethelm et al, *Fuel Cells*, **13** (2013).

8. F. Alenazey et al, *Int. J. Hydrogen Energy.*, **40** (2015).
9. M. Kotisaari et al, *Fuel Cells*, (2016).
10. Elcogen AS/Oy, www.elcogen.com, (accessed 1.4.2017).